


Measurements of Groomed-Jet Substructure of Charm Jets Tagged by D^0 Mesons in Proton-Proton Collisions at $\sqrt{s} = 13$ TeV

S. Acharya *et al.**
(ALICE Collaboration)

 (Received 25 August 2022; revised 13 January 2023; accepted 19 July 2023; published 7 November 2023)

Understanding the role of parton mass and Casimir color factors in the quantum chromodynamics parton shower represents an important step in characterizing the emission properties of heavy quarks. Recent experimental advances in jet substructure techniques have provided the opportunity to isolate and characterize gluon emissions from heavy quarks. In this Letter, the first direct experimental constraint on the charm-quark splitting function is presented, obtained via the measurement of the groomed shared momentum fraction of the first splitting in charm jets, tagged by a reconstructed D^0 meson. The measurement is made in proton-proton collisions at $\sqrt{s} = 13$ TeV, in the low jet transverse-momentum interval of $15 \leq p_T^{\text{jet ch}} < 30$ GeV/ c where the emission properties are sensitive to parton mass effects. In addition, the opening angle of the first perturbative emission of the charm quark, as well as the number of perturbative emissions it undergoes, is reported. Comparisons to measurements of an inclusive-jet sample show a steeper splitting function for charm quarks compared with gluons and light quarks. Charm quarks also undergo fewer perturbative emissions in the parton shower, with a reduced probability of large-angle emissions.

DOI: 10.1103/PhysRevLett.131.192301

In hadronic collisions, quarks and gluons (partons) with high transverse momentum (p_T) and/or large masses are produced in scattering processes involving large momentum transfers. These energetic partons lose their large initial virtuality by emitting partons in a cascade process known as a parton shower, until they eventually form hadrons. Theoretical descriptions of parton showers rely on determining the emission probability of partons, which are described by splitting functions [1,2]. Splitting functions are universal properties of quantum chromodynamics (QCD) that describe how the energy of a parton is shared as it fragments into further partons. The splitting functions of light-flavor (up, down, and strange) quarks and gluons differ due to their different Casimir color factors [2]. For heavy-flavor [charm and beauty with masses of (1.27 ± 0.02) GeV/ c^2 and $4.18^{+0.03}_{-0.02}$ GeV/ c^2 , respectively [3]] quarks the splitting functions are strongly influenced by the large quark mass [4]. As a consequence, the radiation pattern of the parton shower depends on the type of initiating parton.

Experimental access to the parton shower can be gained via measurements involving jets, which are collimated

bunches of hadrons resulting from the fragmentation of partons scattered in the initial stages of collisions. Jets represent a powerful tool for testing perturbative QCD, as their inner structure (substructure) reflects the properties of the underlying parton shower. Measurements of jet substructure have been performed in inclusive jets (with no flavor tagging) to constrain the splitting functions of light quarks and gluons [5–8]. However, an experimentally clean separation of gluon-initiated and quark-initiated jets has remained challenging, with measurements constraining the splitting functions comprising an admixture of the two subsets.

Recent experimental advances in techniques pertaining to the substructure of heavy-flavor jets [9,10] have allowed for the isolation and study of gluon emissions from heavy quarks. This technique has been used to perform a first direct measurement [11] of the dead-cone effect [12] in charm-quark jets. The dead cone corresponds to an angular region along the flight direction of the emitter, with an opening proportional to the ratio of mass to energy of the emitter, within which the probability of emissions is suppressed. The significant size of this region for low-energy heavy-flavor quarks gives rise to mass-dependent effects in the parton shower. In addition to the sensitivity to these mass effects in QCD, heavy-flavor jets represent an experimentally enhanced quark-initiated jet sample, which can be further used to constrain the flavor-dependent properties of QCD emissions arising from different Casimir color factors.

*Full author list given at the end of the article.

Published by the American Physical Society under the terms of the [Creative Commons Attribution 4.0 International license](https://creativecommons.org/licenses/by/4.0/). Further distribution of this work must maintain attribution to the author(s) and the published article's title, journal citation, and DOI.

In this Letter, the first measurement directly constraining the charm-quark splitting function is reported. This requires access to perturbative splittings (the splitting scale is much larger than the QCD scale) of the charm quark, where the shared momentum fraction of the splittings maps onto the analytical splitting function [13–15]. Additionally, measurements of the opening angle of these emissions, as well as the number of perturbative emissions in charm jets, are reported. Measurements of these two observables have also been reported for inclusive jets [6–8,16,17], with the opening angle calculated at next-to-leading logarithmic accuracy [18]. The measurements reported in this work are made in the low jet transverse-momentum interval of $15 \leq p_T^{\text{jet ch}} < 30 \text{ GeV}/c$, where mass effects are expected to play a role in the fragmentation of the charm quark and the inclusive sample is mainly comprised of gluon-initiated jets.

Once jets have been identified from the sample of charged particles (reconstructed as tracks) in p - p collisions, using the anti- k_T algorithm [19], track-based jet-substructure observables can be constructed from the jet constituents. To reconstruct the chain of emissions (splitting tree) inside a jet, the jet constituents can be reclustered with the Cambridge–Aachen (C/A) algorithm [20], which is well suited to jet substructure studies because it follows the angular ordering of emissions in QCD [1] by clustering the jet constituents based on their angular distance. By following a branch along the splitting tree returned by the reclustering procedure, a sequence of emissions can be studied [21].

Charm jets are identified by the presence of a reconstructed D^0 meson amongst their constituents. The full reconstruction of the $D^0 \rightarrow K^- \pi^+$ decay allows for the replacement of the D^0 decay products with the four-momentum of the D^0 meson, prior to jet clustering. This ensures that the full D^0 -meson momentum is contained within the jet cone. As the charm flavor is conserved throughout the jet evolution, the charm quark can be traced as it dynamically evolves in the showering process, by following the branch containing the D^0 meson through the splitting tree [9].

To reduce the contribution of nonperturbative effects and increase sensitivity to perturbative emissions [22], the soft drop grooming procedure [23] is applied, which only selects particular splittings of interest along the followed branch. To do this, each splitting along this branch is tested against the soft drop condition, as given by

$$z \equiv \frac{\min(p_{T,1}, p_{T,2})}{p_{T,1} + p_{T,2}} > z_{\text{cut}} \left(\frac{\Delta R_{1,2}}{R} \right)^\beta, \quad (1)$$

where $p_{T,1}$ and $p_{T,2}$ are the transverse momenta of the leading and subleading prongs of the splitting, respectively, and R is the jet resolution parameter. The grooming behavior is determined by the parameters z_{cut} and β , which control the interplay between the shared momentum

fraction, z , and the aperture angle between the prongs, $\Delta R_{1,2} \equiv \sqrt{(y_1 - y_2)^2 + (\varphi_1 - \varphi_2)^2}$, where y and φ are the rapidity and azimuth of prongs 1 and 2, respectively. In this work, values of $z_{\text{cut}} = 0.1$ and $\beta = 0$ are chosen, such that the soft drop condition is satisfied if the subleading prong carries at least 10% of the sum of the transverse momenta of the prongs, enriching the selection with perturbative splittings.

Two groomed substructure observables are constructed against the first splitting that satisfies the soft drop condition: $z_g = z$ and $R_g = \Delta R_{1,2}$, as given in Eq. (1). For the given choices of grooming parameters, the shared momentum fraction z_g converges to the QCD splitting function at sufficiently high jet energies [13]. As the emissions are angular ordered, the groomed emission angle R_g characterizes the widest emission in the splitting tree which passes the soft drop condition and sets the geometrical scale of the jet. This observable is expected to be sensitive to the dead cone of the charm quark at small angles, whilst emissions from gluons, which have a larger Casimir color factor, are expected to dominate the large-angle region [24,25]. The number of emissions of the charm quark satisfying the soft drop condition, n_{SD} , is also measured by evaluating all splittings along the branch containing the D^0 meson. This strongly correlates to the number of perturbative emissions of the charm quark.

The data were collected using the ALICE apparatus at the LHC, during the years 2016, 2017, and 2018. Information about the detector configuration and performance can be found in Refs. [26,27]. The main detector systems used for this work were the central barrel detectors, located at $|\eta| < 0.9$ within a solenoidal magnet and used for charged-particle tracking and identification. These include the inner tracking system, the time projection chamber, and the time-of-flight detector. The V0 detector, consisting of two scintillator arrays located at pseudorapidities of $2.8 < \eta < 5.1$ and $-3.7 < \eta < -1.7$, was used for the trigger and event selections. Minimum-bias events were selected by requiring a signal above a given threshold in both V0 counters. The analyzed data sample consisted of about 1.7×10^9 p - p collisions at a center-of-mass energy of $\sqrt{s} = 13 \text{ TeV}$, corresponding to an integrated luminosity of $\mathcal{L}_{\text{int}} = 29 \text{ nb}^{-1}$.

The D^0 mesons were reconstructed in the $D^0 p_T$ interval of $5 \leq p_T^{D^0} < 30 \text{ GeV}/c$, through the $D^0 \rightarrow K^- \pi^+$ (and charge conjugate) decay channel with a branching ratio of $(3.95 \pm 0.03)\%$ [3]. Background candidates, built from pairs of tracks not corresponding to a D^0 decay, were suppressed by applying geometrical selections on the displaced-decay-vertex topology, as well as particle identification on the decay-particle tracks [28]. The D^0 decay daughters were replaced in the event by the D^0 -meson four-momentum, which was obtained by summing the four-momenta of these decay daughters. Jet finding was then

performed using the `FastJet` package [29], with the anti- k_T algorithm, a resolution parameter of $R = 0.4$ and the E -scheme recombination. The inputs to the jet finder consisted of tracks of charged particles with $p_T \geq 0.15$ GeV/ c and the reconstructed D^0 meson candidate. The full set of quality selections applied to the tracks, including the D^0 -meson candidate decay tracks, is given in Ref. [30]. The jets were required to be fully contained within the central barrel acceptance, by imposing a pseudorapidity selection of $|\eta| < 0.5$ on the jet axis. For every D^0 meson candidate in an event, jet finding was performed independently, with only the two tracks forming that particular candidate replaced with the sum of their four-momenta prior to the jet finding pass. Once jet finding had been performed, the D^0 -tagged jet constituents were reclustered using the C/A algorithm, and the z_g , R_g , and n_{SD} observables were calculated for each jet. The contribution to the three observable distributions from jets tagged by background D^0 candidates that survived the selection was removed via a sideband subtraction procedure, as detailed in Refs. [30,31]. This procedure provides the true D^0 -tagged jet observable distributions in intervals of $p_T^{D^0}$.

Each of these background-subtracted distributions was scaled by the selection and reconstruction efficiency of prompt (charm showering) D^0 -tagged jets, estimated in $p_T^{D^0}$ intervals, from Monte Carlo (MC) simulations using `PYTHIA 8.243` [32–34] and `GEANT 3` [35]. The efficiency-corrected distributions were summed over the full $p_T^{D^0}$ range considered for the analysis. In order to study emissions in the charm-quark shower, the contribution from nonprompt D^0 mesons (feed-down contribution), originating from the decay of beauty hadrons, was estimated using `POWHEG` [36] simulations with `PYTHIA 6.425` [33] showering and decays implemented through the `EvtGen` package [37]. It was then subtracted from the measured distributions. The magnitude of this nonprompt contribution ranged from 20% to 40% in most of the z_g , R_g , and n_{SD} intervals considered in the analysis. The $p_T^{\text{jet ch}}$ distributions and each prompt D^0 -tagged jet substructure observable were simultaneously corrected for detector effects via a two-dimensional unfolding, using the iterative Bayesian unfolding algorithm with four iterations [38].

The z_g , R_g , and n_{SD} jet observables were also measured for inclusive jets. To allow for direct comparisons with the heavy-flavor results, the constraint on the Q^2 value of the parton scattering implied by the selection of D^0 mesons with $p_T^{D^0} \geq 5$ GeV/ c was mimicked for inclusive jets, by requiring a leading track with $p_T \geq 5.33$ GeV/ c . This corresponds to the p_T of a charged pion with the same transverse mass as a D^0 meson with $p_T^{D^0} = 5$ GeV/ c . In addition, during the grooming procedure, the hardest branch of the splitting tree was followed. In the heavy-flavor sample, following the hardest branch was found to coincide with following the branch containing the D^0 , in

over 99% of cases. The inclusive-jet distributions were then corrected for detector effects via the same unfolding procedure as in the D^0 -tagged jet case.

Systematic uncertainties related to the reconstruction and identification of prompt D^0 -tagged jets were studied. The stability of the selections applied to the D^0 -meson candidates were estimated by loosening and tightening the topological and particle identification criteria used to identify the D^0 decays. The uncertainty pertaining to the signal extraction procedure was estimated by changing the fitting parameters on the invariant-mass fits, as well as the widths of the signal and sideband regions used for the sideband subtraction procedure. The uncertainty on the D^0 feed-down estimation was obtained by varying the renormalization and factorization scales, as well as the mass of the beauty quark, in the `POWHEG` simulations [39]. The uncertainty on the jet energy resolution was estimated by artificially reducing the tracking efficiency used to generate the unfolding response matrix by 4%, in line with the tracking efficiency uncertainty of the ALICE detector. Finally, the uncertainty associated with the unfolding procedure was obtained by varying the number of iterations, the choice of prior, and the ranges of the response matrix. Additionally, variations of the fragmentation properties of the MC simulation used to construct the response matrix were also included. These were obtained by reweighting the response matrix based on the value of the jet-angularity observable [40] ($\kappa = 1$ and $\beta = 1$) calculated for each entry, as this observable is sensitive to the transverse momentum and angular distribution of all hadrons in the jet. The weights were devised such that the reweighting procedure transformed the angularity distribution at generator level of the D^0 -tagged jets in the response matrix, to match that of a simulated inclusive-jet distribution.

The dominant contributions in most of the intervals resulted from variations of the topological selections, signal extraction, and feed-down subtraction. For the feed-down subtraction uncertainty, the maximum negative and the maximum positive deviations were taken, respectively. For each of the other variation categories, the root mean square of deviations from the central values was calculated and assigned as a systematic uncertainty, which was then symmetrized around the central value. The uncertainties from all categories were then added in quadrature to obtain the full systematic uncertainty. The total systematic uncertainties range from 7% to 77%, from 9% to 12%, and from 5% to 59% for the D^0 -tagged jet z_g , R_g , and n_{SD} distributions, respectively.

The systematic uncertainties for the inclusive-jet distributions were estimated by performing variations of the tracking efficiency and unfolding, in the same way as in the D^0 -tagged jet case. In addition, the p_T selection on the leading track of the jet was also varied in line with the track p_T resolution of the D^0 -decay tracks. The total systematic uncertainties range from 1.4% to 4.3%, from 2.2% to 5.7%,

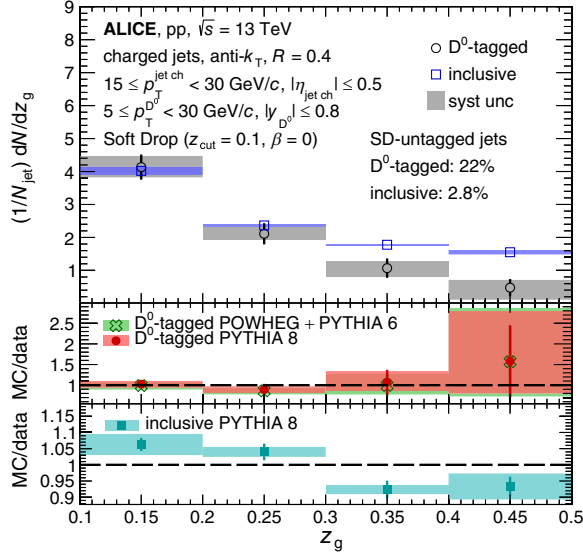


FIG. 1. The z_g distribution of prompt D^0 -tagged jets compared to that of inclusive jets for $15 \leq p_T^{\text{jet ch}} < 30$ GeV/c in p - p collisions at $\sqrt{s} = 13$ TeV, normalized to the total number of jets. Model-data ratios are shown in the bottom panels for PYTHIA 8 [32–34] and POWHEG [36] + PYTHIA 6 [33] simulations.

and from 3.3% to 8.1% for the inclusive-jet z_g , R_g , and n_{SD} distributions, respectively.

The first measurement mapping onto the charm-quark splitting function is reported via the z_g distribution in Fig. 1, for charm jets tagged by a prompt D^0 meson. The R_g and n_{SD} distributions are shown in the left and right panels of Fig. 2, respectively. These distributions are fully corrected

for detector effects and are reported in the jet transverse-momentum interval of $15 \leq p_T^{\text{jet ch}} < 30$ GeV/c. Each charm-tagged jet measurement is accompanied by a measurement of an inclusive-jet sample in the same kinematic interval, also fully corrected for detector effects. Both the charm-tagged jet and inclusive-jet distributions are normalized to the total number of jets in each respective category, irrespective of whether they had a splitting passing the soft drop condition or not. In this way, the distributions are sensitive to the proportion of jets that do not have any splittings passing the soft drop condition, denoted as the SD untagged fraction. These fractions are 22% and 2.8%, in the charm-tagged jet and inclusive-jet samples, respectively. Both samples are compared to PYTHIA 8 simulations and also to POWHEG + PYTHIA 6 simulations for the charm-tagged jets. The ratios of predicted distributions from parton-shower models to the measured distributions are also shown in the bottom panels of Figs. 1 and 2. A comparison of the measured z_g distribution to analytical calculations performed in the soft-collinear effective theory (SCET) framework [41,42] can be found in the Supplemental Material [43].

The z_g distributions show that charm-tagged jets have significantly fewer symmetric splittings (large z_g values), compared with inclusive jets. This is consistent with theoretical predictions [10] of the role of mass effects in the QCD splitting function. The R_g distribution for charm quarks shows a reduction at large angles compared with inclusive jets. This can be due to the differences between quark and gluon fragmentation, with the gluon-dominated inclusive sample expected to feature larger-angle

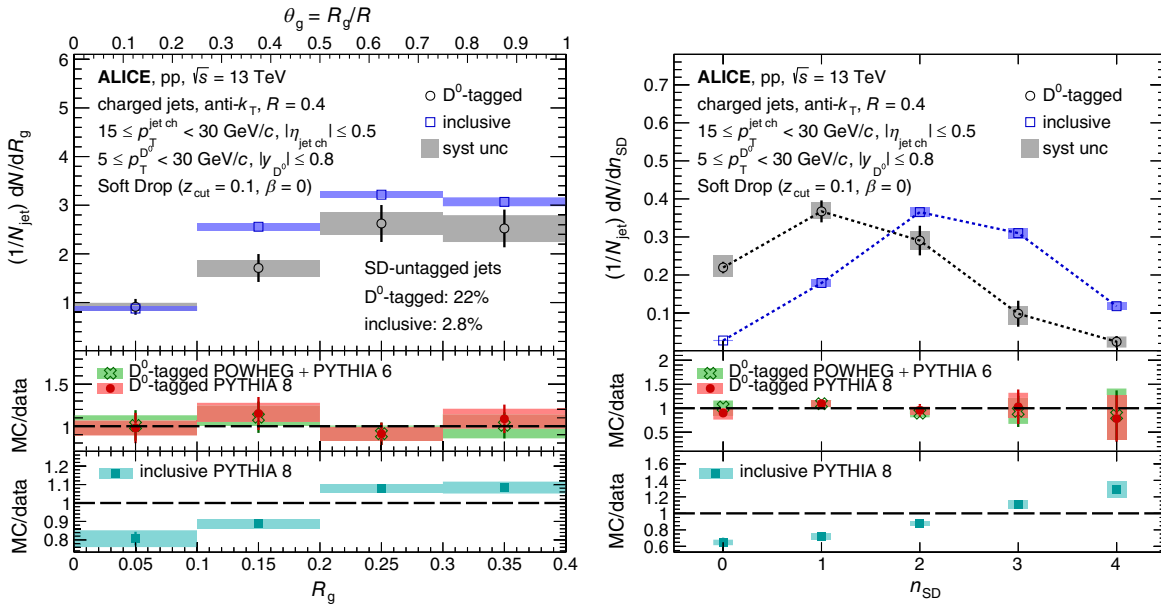


FIG. 2. The R_g (left) and n_{SD} (right) distributions of prompt D^0 -tagged jets compared to those of inclusive jets for $15 \leq p_T^{\text{jet ch}} < 30$ GeV/c in p - p collisions at $\sqrt{s} = 13$ TeV. Model-data ratios are shown in the bottom panels for PYTHIA 8 [32–34] and POWHEG [36] + PYTHIA 6 [33] simulations.

perturbative emissions. The charm and inclusive-jet distributions are consistent at small R_g . This could be due to an interplay between the dead-cone effect, which suppresses small-angle emissions from the charm quark, and the more abundant emissions from quarks compared with gluons at small angles, as gluons lose more of their initial virtuality through larger-angle emissions. The n_{SD} distribution shows a significant shift to smaller values for the charm-tagged jets [$\langle n_{SD} \rangle = 1.34 \pm 0.08(\text{stat.}) \pm 0.07(\text{syst.})$] compared with inclusive jets [$\langle n_{SD} \rangle = 2.31 \pm 0.01(\text{stat.}) \pm 0.02(\text{syst.})$]. This indicates that, compared with light and massless partons, charm quarks on average emit fewer gluons with a large enough p_T to pass the soft drop condition in the showering process. This is consistent with the expectation from the presence of a dead cone for charm quarks, which results in a harder fragmentation of charm quarks compared with light quarks and gluons.

For all three observables, both the PYTHIA 8 and POWHEG + PYTHIA 6 predictions for charm-quark jets describe the measurements within uncertainties. For the more precise inclusive measurements, PYTHIA 8 exhibits some tension, particularly for the n_{SD} observable. This may be partially due to the poorly constrained quark and gluon fractions in the inclusive sample at low $p_T^{\text{jet ch}}$. In contrast, as the D^0 -tagged jets represent a quark-enriched sample, the comparison of the shower generators to data is less reliant on this fraction and can instead be used to more accurately study the mechanisms underpinning the shower properties.

The measurement of the groomed shared momentum fraction z_g of charm-tagged jets, reported in this Letter, represents the first direct experimental constraint of the splitting function of heavy-flavor quarks. The z_g distribution appears steeper than that of light quarks and gluons, with a suppressed probability of symmetric emissions. Measurements of the number of splittings passing the soft drop condition as well as the emission angle of the first of these splittings, show that heavy-flavor quarks on average have fewer perturbative emissions compared with light quarks and gluons, with a lower probability of these emissions occurring at large angles. These different characteristics for heavy-quark emissions, compared with light quarks and gluons, constrain the roles of quark mass and Casimir color factors in the parton shower, which are different between the two samples. The upgraded ALICE detector in the LHC Run 3 will extend this measurement to jets tagged with a fully reconstructed beauty meson [44]. Direct comparison of the two quark-enriched samples of charm-tagged and beauty-tagged jets will enable the isolation of mass effects from the effects due to Casimir color factors. The larger projected integrated luminosity in Run 3 will also allow us to extend the charm-tagged to inclusive-jet comparisons to higher $p_T^{\text{jet ch}}$, where mass effects become negligible and the remaining impact of the Casimir color factors can be cleanly studied.

The ALICE Collaboration would like to thank all its engineers and technicians for their invaluable contributions to the construction of the experiment and the CERN accelerator teams for the outstanding performance of the LHC complex. The ALICE Collaboration gratefully acknowledges the resources and support provided by all Grid centers and the Worldwide LHC Computing Grid (WLCG) Collaboration. The ALICE Collaboration acknowledges the following funding agencies for their support in building and running the ALICE detector: A. I. Alikhanyan National Science Laboratory (Yerevan Physics Institute) Foundation (ANSL), State Committee of Science and World Federation of Scientists (WFS), Armenia; Austrian Academy of Sciences, Austrian Science Fund (FWF): [M 2467-N36] and Nationalstiftung für Forschung, Technologie und Entwicklung, Austria; Ministry of Communications and High Technologies, National Nuclear Research Center, Azerbaijan; Conselho Nacional de Desenvolvimento Científico e Tecnológico (CNPq), Financiadora de Estudos e Projetos (Finep), Fundação de Amparo à Pesquisa do Estado de São Paulo (FAPESP) and Universidade Federal do Rio Grande do Sul (UFRGS), Brazil; Bulgarian Ministry of Education and Science, within the National Roadmap for Research Infrastructures 2020–2027 (object CERN), Bulgaria; Ministry of Education of China (MOEC), Ministry of Science & Technology of China (MSTC) and National Natural Science Foundation of China (NSFC), China; Ministry of Science and Education and Croatian Science Foundation, Croatia; Centro de Aplicaciones Tecnológicas y Desarrollo Nuclear (CEADEN), Cubaenergía, Cuba; Ministry of Education, Youth and Sports of the Czech Republic, Czech Republic; The Danish Council for Independent Research | Natural Sciences, the VILLUM FONDEN and Danish National Research Foundation (DNRF), Denmark; Helsinki Institute of Physics (HIP), Finland; Commissariat à l’Energie Atomique (CEA) and Institut National de Physique Nucléaire et de Physique des Particules (IN2P3) and Centre National de la Recherche Scientifique (CNRS), France; Bundesministerium für Bildung und Forschung (BMBF) and GSI Helmholtzzentrum für Schwerionenforschung GmbH, Germany; General Secretariat for Research and Technology, Ministry of Education, Research and Religions, Greece; National Research, Development and Innovation Office, Hungary; Department of Atomic Energy Government of India (DAE), Department of Science and Technology, Government of India (DST), University Grants Commission, Government of India (UGC) and Council of Scientific and Industrial Research (CSIR), India; National Research and Innovation Agency—BRIN, Indonesia; Istituto Nazionale di Fisica Nucleare (INFN), Italy; Japanese Ministry of Education, Culture, Sports, Science and Technology (MEXT) and Japan Society for the Promotion of Science (JSPS) KAKENHI, Japan; Consejo

Nacional de Ciencia (CONACYT) y Tecnología, through Fondo de Cooperación Internacional en Ciencia y Tecnología (FONCICYT) and Dirección General de Asuntos del Personal Académico (DGAPA), Mexico; Nederlandse Organisatie voor Wetenschappelijk Onderzoek (NWO), Netherlands; The Research Council of Norway, Norway; Commission on Science and Technology for Sustainable Development in the South (COMSATS), Pakistan; Pontificia Universidad Católica del Perú, Peru; Ministry of Education and Science, National Science Centre and WUT ID-UB, Poland; Korea Institute of Science and Technology Information and National Research Foundation of Korea (NRF), Republic of Korea; Ministry of Education and Scientific Research, Institute of Atomic Physics, Ministry of Research and Innovation and Institute of Atomic Physics and University Politehnica of Bucharest, Romania; Ministry of Education, Science, Research and Sport of the Slovak Republic, Slovakia; National Research Foundation of South Africa, South Africa; Swedish Research Council (VR) and Knut & Alice Wallenberg Foundation (KAW), Sweden; European Organization for Nuclear Research, Switzerland; Suranaree University of Technology (SUT), National Science and Technology Development Agency (NSTDA), Thailand Science Research and Innovation (TSRI) and National Science, Research and Innovation Fund (NSRF), Thailand; Turkish Energy, Nuclear and Mineral Research Agency (TENMAK), Turkey; National Academy of Sciences of Ukraine, Ukraine; Science and Technology Facilities Council (STFC), United Kingdom; National Science Foundation of the United States of America (NSF) and United States Department of Energy, Office of Nuclear Physics (DOE NP), United States of America. In addition, individual groups or members have received support from Marie Skłodowska Curie, European Research Council, Strong 2020—Horizon 2020 (Grants No. 950692, No. 824093, No. 896850), European Union; Academy of Finland (Center of Excellence in Quark Matter) (Grants No. 346327, No. 346328), Finland; Programa de Apoyos para la Superación del Personal Académico, UNAM, Mexico.

-
- [1] Y. L. Dokshitzer, V. A. Khoze, A. H. Mueller, and S. I. Troian, *Basics of Perturbative QCD* (Ed. Frontieres, 1991).
 [2] G. Altarelli and G. Parisi, Asymptotic freedom in parton language, *Nucl. Phys.* **B126**, 298 (1977).
 [3] P. A. Zyla *et al.* (Particle Data Group Collaboration), Review of particle physics, *Prog. Theor. Exp. Phys.* **2020**, 083C01 (2020), and 2021 update.
 [4] E. G. de Oliveira, A. D. Martin, M. G. Ryskin, and A. G. Shuvaev, Treatment of heavy quarks in QCD, *Eur. Phys. J. C* **73**, 2616 (2013).

- [5] A. M. Sirunyan *et al.* (CMS Collaboration), Measurement of the Splitting Function in pp and Pb–Pb Collisions at $\sqrt{s_{NN}} = 5.02$ TeV, *Phys. Rev. Lett.* **120**, 142302 (2018).
 [6] S. Acharya *et al.* (ALICE Collaboration), Measurement of the Groomed Jet Radius and Momentum Splitting Fraction in pp and Pb–Pb Collisions at $\sqrt{s_{NN}} = 5.02$ TeV, *Phys. Rev. Lett.* **128**, 102001 (2022).
 [7] G. Aad *et al.* (ATLAS Collaboration), Measurement of soft-drop jet observables in pp collisions with the ATLAS detector at $\sqrt{s} = 13$ TeV, *Phys. Rev. D* **101**, 052007 (2020).
 [8] J. Adam *et al.* (STAR Collaboration), Measurement of groomed jet substructure observables in p + p collisions at $\sqrt{s} = 200$ GeV with STAR, *Phys. Lett. B* **811**, 135846 (2020).
 [9] L. Cunqueiro and M. Płoskoń, Searching for the dead cone effects with iterative declustering of heavy-flavor jets, *Phys. Rev. D* **99**, 074027 (2019).
 [10] P. Ilten, N. L. Rodd, J. Thaler, and M. Williams, Disentangling heavy flavor at colliders, *Phys. Rev. D* **96**, 054019 (2017).
 [11] S. Acharya *et al.* (ALICE Collaboration), Direct observation of the dead-cone effect in quantum chromodynamics, *Nature (London)* **605**, 440 (2022).
 [12] Y. L. Dokshitzer, V. A. Khoze, and S. I. Troian, On specific QCD properties of heavy quark fragmentation ('dead cone'), *J. Phys. G* **17**, 1602 (1991).
 [13] A. Larkoski, S. Marzani, J. Thaler, A. Tripathy, and W. Xue, Exposing the QCD Splitting Function with CMS Open Data, *Phys. Rev. Lett.* **119**, 132003 (2017).
 [14] A. J. Larkoski, S. Marzani, and J. Thaler, Sudakov safety in perturbative QCD, *Phys. Rev. D* **91**, 111501(R) (2015).
 [15] P. Cal, K. Lee, F. Ringer, and W. J. Waalewijn, The soft drop momentum sharing fraction z_g beyond leading-logarithmic accuracy, *Phys. Lett. B* **833**, 137390 (2022).
 [16] S. Acharya *et al.* (ALICE Collaboration), Exploration of jet substructure using iterative declustering in pp and Pb–Pb collisions at LHC energies, *Phys. Lett. B* **802**, 135227 (2020).
 [17] S. Acharya *et al.* (ALICE Collaboration), Measurements of the groomed jet radius and momentum splitting fraction with the soft drop and dynamical grooming algorithms in pp collisions at $\sqrt{s} = 5.02$ TeV, *J. High Energy Phys.* **05** (2023) 244.
 [18] Z.-B. Kang, K. Lee, X. Liu, D. Neill, and F. Ringer, The soft drop groomed jet radius at NLL, *J. High Energy Phys.* **02** (2020) 054.
 [19] M. Cacciari, G. P. Salam, and G. Soyez, The anti- k_t jet clustering algorithm, *J. High Energy Phys.* **04** (2008) 063.
 [20] Y. L. Dokshitzer, G. D. Leder, S. Moretti, and B. R. Webber, Better jet clustering algorithms, *J. High Energy Phys.* **08** (1997) 001.
 [21] F. A. Dreyer, G. P. Salam, and G. Soyez, The Lund jet plane, *J. High Energy Phys.* **12** (2018) 064.
 [22] S. Acharya *et al.* (ALICE Collaboration), Measurements of the groomed and ungroomed jet angularities in pp collisions at $\sqrt{s} = 5.02$ TeV, *J. High Energy Phys.* **05** (2022) 061.
 [23] A. J. Larkoski, S. Marzani, G. Soyez, and J. Thaler, Soft drop, *J. High Energy Phys.* **05** (2014) 146.

- [24] P. D. Acton *et al.* (OPAL Collaboration), A study of differences between quark and gluon jets using vertex tagging of quark jets, *Z. Phys. C* **58**, 387 (1993).
- [25] A. Tumasyan *et al.* (CMS Collaboration), Study of quark and gluon jet substructure in Z + jet and dijet events from pp collisions, *J. High Energy Phys.* **01** (2022) 188.
- [26] K. Aamodt *et al.* (ALICE Collaboration), The ALICE experiment at the CERN LHC, *J. Instrum.* **3**, S08002 (2008).
- [27] B. Abelev *et al.* (ALICE Collaboration), Performance of the ALICE experiment at the CERN LHC, *Int. J. Mod. Phys. A* **29**, 1430044 (2014).
- [28] S. Acharya *et al.* (ALICE Collaboration), Measurement of the production of charm jets tagged with D^0 mesons in pp collisions at $\sqrt{s} = 7$ TeV, *J. High Energy Phys.* **08** (2019) 133.
- [29] M. Cacciari, G. P. Salam, and G. Soyez, FastJet user manual, *Eur. Phys. J. C* **72**, 1896 (2012).
- [30] S. Acharya *et al.* (ALICE Collaboration), Measurement of the production of charm jets tagged with D^0 mesons in pp collisions at $\sqrt{s} = 5.02$ and 13 TeV, *J. High Energy Phys.* **06** (2023) 133.
- [31] S. Acharya *et al.* (ALICE Collaboration), Groomed jet substructure measurements of charm jets tagged with D^0 mesons in pp collisions at $\sqrt{s} = 13$ TeV, Report No. ALICE-PUBLIC-2020-002, 2020, <https://cds.cern.ch/record/2719005>.
- [32] P. Skands, S. Carrazza, and J. Rojo, Tuning PYTHIA 8.1: The Monash 2013 tune, *Eur. Phys. J. C* **74**, 3024 (2014).
- [33] T. Sjöstrand, S. Mrenna, and P. Z. Skands, PYTHIA 6.4 physics and manual, *J. High Energy Phys.* **05** (2006) 026.
- [34] T. Sjöstrand, S. Ask, J. R. Christiansen, R. Corke, N. Desai, P. Ilten, S. Mrenna, S. Prestel, C. O. Rasmussen, and P. Z. Skands, An introduction to PYTHIA 8.2, *Comput. Phys. Commun.* **191**, 159 (2015).
- [35] R. Brun, F. Bruyant, M. Maire, A. C. McPherson, and P. Zanzarini, GEANT 3: User's guide GEANT 3.10, GEANT 3.11; rev. version (CERN, Geneva, 1987), <https://cds.cern.ch/record/1119728>.
- [36] S. Alioli, P. Nason, C. Oleari, and E. Re, A general framework for implementing NLO calculations in shower Monte Carlo programs: The POWHEG BOX, *J. High Energy Phys.* **06** (2010) 043.
- [37] D. J. Lange, The EvtGen particle decay simulation package, *Nucl. Instrum. Methods Phys. Res., Sect. A* **462**, 152 (2001).
- [38] G. D'Agostini, A multidimensional unfolding method based on Bayes' theorem, *Nucl. Instrum. Methods Phys. Res., Sect. A* **362**, 487 (1995).
- [39] M. Cacciari, P. Nason, and R. Vogt, QCD Predictions for Charm and Bottom Production at RHIC, *Phys. Rev. Lett.* **95**, 122001 (2005).
- [40] A. J. Larkoski, J. Thaler, and W. J. Waalewijn, Gaining (mutual) information about quark/gluon discrimination, *J. High Energy Phys.* **11** (2014) 129.
- [41] H. T. Li and I. Vitev, Inverting the mass hierarchy of jet quenching effects with prompt b-jet substructure, *Phys. Lett. B* **793**, 259 (2019).
- [42] H. T. Li, Z. L. Liu, and I. Vitev, Heavy flavor jet production and substructure in electron–nucleus collisions, *Phys. Lett. B* **827**, 137007 (2022).
- [43] See Supplemental Material at <http://link.aps.org/supplemental/10.1103/PhysRevLett.131.192301> for additional data with model comparisons.
- [44] S. Acharya *et al.* (ALICE Collaboration), Future high-energy pp programme with ALICE, Report No. ALICE-PUBLIC-2020-005, <https://cds.cern.ch/record/2724925>.

S. Acharya¹²⁵, D. Adamová⁸⁶, A. Adler⁶⁹, G. Aglieri Rinella³², M. Agnello²⁹, N. Agrawal⁵⁰, Z. Ahammed¹³², S. Ahmad¹⁵, S. U. Ahn⁷⁰, I. Ahuja³⁷, A. Akindinov¹⁴⁰, M. Al-Turany⁹⁸, D. Aleksandrov¹⁴⁰, B. Alessandro⁵⁵, H. M. Alfanda⁶, R. Alfaro Molina⁶⁶, B. Ali¹⁵, Y. Ali¹³, A. Alici²⁵, N. Alizadehvandchali¹¹⁴, A. Alkin³², J. Alme²⁰, G. Alocco⁵¹, T. Alt⁶³, I. Altsybeev¹⁴⁰, M. N. Anaam⁶, C. Andrei⁴⁵, A. Andronic¹³⁵, V. Anguelov⁹⁵, F. Antinori⁵³, P. Antonioli⁵⁰, C. Anuj¹⁵, N. Apadula⁷⁴, L. Aphecetche¹⁰⁴, H. Appelshäuser⁶³, C. Arata⁷³, S. Arcelli²⁵, M. Aresti⁵¹, R. Arnaldi⁵⁵, I. C. Arsene¹⁹, M. Arslandok¹³⁷, A. Augustinus³², R. Averbeck⁹⁸, M. D. Azmi¹⁵, A. Badalà⁵², Y. W. Baek⁴⁰, X. Bai¹¹⁸, R. Bailhache⁶³, Y. Bailung⁴⁷, R. Bala⁹¹, A. Balbino²⁹, A. Baldisseri¹²⁸, B. Balis², D. Banerjee⁴, Z. Banoo⁹¹, R. Barbera²⁶, F. Barile³¹, L. Barioglio⁹⁶, M. Barlou⁷⁸, G. G. Barnaföldi¹³⁶, L. S. Barnby⁸⁵, V. Barret¹²⁵, L. Barreto¹¹⁰, C. Bartels¹¹⁷, K. Barth³², E. Bartsch⁶³, F. Baruffaldi²⁷, N. Bastid¹²⁵, S. Basu⁷⁵, G. Batigne¹⁰⁴, D. Battistini⁹⁶, B. Batyunya¹⁴¹, D. Bauri⁴⁶, J. L. Bazo Alba¹⁰², I. G. Bearden⁸³, C. Beattie¹³⁷, P. Becht⁹⁸, D. Behera⁴⁷, I. Belikov¹²⁷, A. D. C. Bell Hechavarria¹³⁵, F. Bellini²⁵, R. Bellwied¹¹⁴, S. Belokurova¹⁴⁰, V. Belyaev¹⁴⁰, G. Bencedi^{64,136}, S. Beole²⁴, A. Bercuci⁴⁵, Y. Berdnikov¹⁴⁰, A. Berdnikova⁹⁵, L. Bergmann⁹⁵, M. G. Besoiu⁶², L. Betev³², P. P. Bhaduri¹³², A. Bhasin⁹¹, M. A. Bhat⁴, B. Bhattacharjee⁴¹, L. Bianchi²⁴, N. Bianchi⁴⁸, J. Bielčík³⁵, J. Bielčíková⁸⁶, J. Biernat¹⁰⁷, A. P. Bigot¹²⁷, A. Bilandzic⁹⁶, G. Biro¹³⁶, S. Biswas⁴, N. Bize¹⁰⁴, J. T. Blair¹⁰⁸, D. Blau¹⁴⁰, M. B. Blidaru⁹⁸, N. Bluhme³⁸, C. Blume⁶³, G. Boca^{21,54}, F. Bock⁸⁷, T. Bodova²⁰, A. Bogdanov¹⁴⁰, S. Boi²², J. Bok⁵⁷, L. Boldizsár¹³⁶, A. Bolozdynya¹⁴⁰, M. Bombara³⁷, P. M. Bond³², G. Bonomi^{54,131}, H. Borel¹²⁸, A. Borissov¹⁴⁰, H. Bossi¹³⁷, E. Botta²⁴, Y. E. M. Bouziani⁶³, L. Bratrud⁶³, P. Braun-Munzinger⁹⁸, M. Bregant¹¹⁰, M. Broz³⁵, G. E. Bruno^{31,97}, M. D. Buckland¹¹⁷, D. Budnikov¹⁴⁰, H. Buesching⁶³, S. Bufalino²⁹

- O. Bugnon,¹⁰⁴ P. Buhler,¹⁰³ Z. Buthelezi,^{67,121} J. B. Butt,¹³ S. A. Bysiak,¹⁰⁷ M. Cai,⁶ H. Caines,¹³⁷ A. Caliva,⁹⁸
E. Calvo Villar,¹⁰² J. M. M. Camacho,¹⁰⁹ P. Camerini,²³ F. D. M. Canedo,¹¹⁰ M. Carabas,¹²⁴ F. Carnesecchi,³²
R. Caron,¹²⁶ J. Castillo Castellanos,¹²⁸ F. Catalano,^{24,29} C. Ceballos Sanchez,¹⁴¹ I. Chakaberia,⁷⁴
P. Chakraborty,⁴⁶ S. Chandra,¹³² S. Chapeland,³² M. Chartier,¹¹⁷ S. Chattopadhyay,¹³² S. Chattopadhyay,¹⁰⁰
T. G. Chavez,⁴⁴ T. Cheng,⁶ C. Cheshkov,¹²⁶ B. Cheynis,¹²⁶ V. Chibante Barroso,³² D. D. Chinellato,¹¹¹
E. S. Chizzali,^{96,b} J. Cho,⁵⁷ S. Cho,⁵⁷ P. Chochula,³² P. Christakoglou,⁸⁴ C. H. Christensen,⁸³ P. Christiansen,⁷⁵
T. Chujo,¹²³ M. Ciacco,²⁹ C. Cicalo,⁵¹ L. Cifarelli,²⁵ F. Cindolo,⁵⁰ M. R. Ciupek,⁹⁸ G. Clai,^{50,c} F. Colamaria,⁴⁹
J. S. Colburn,¹⁰¹ D. Colella,^{31,97} M. Colocci,³² M. Concas,^{55,d} G. Conesa Balbastre,⁷³ Z. Conesa del Valle,⁷²
G. Contin,²³ J. G. Contreras,³⁵ M. L. Coquet,¹²⁸ T. M. Cormier,^{87,a} P. Cortese,^{55,130} M. R. Cosentino,¹¹²
F. Costa,³² S. Costanza,^{21,54} J. Crkovská,⁹⁵ P. Crochet,¹²⁵ R. Cruz-Torres,⁷⁴ E. Cuautele,⁶⁴ P. Cui,⁶ L. Cunqueiro,⁸⁷
A. Dainese,⁵³ M. C. Danisch,⁹⁵ A. Danu,⁶² P. Das,⁸⁰ P. Das,⁴ S. Das,⁴ A. R. Dash,¹³⁵ S. Dash,⁴⁶
R. M. H. David,⁴⁴ A. De Caro,²⁸ G. de Cataldo,⁴⁹ J. de Cuveland,³⁸ A. De Falco,²² D. De Gruttola,²⁸
N. De Marco,⁵⁵ C. De Martin,²³ S. De Pasquale,²⁸ S. Deb,⁴⁷ R. J. Debski,² K. R. Deja,¹³³ R. Del Grande,⁹⁶
L. Dello Stritto,²⁸ W. Deng,⁶ P. Dhankher,¹⁸ D. Di Bari,³¹ A. Di Mauro,³² R. A. Diaz,^{7,141} T. Dietel,¹¹³
Y. Ding,^{6,126} R. Divià,³² D. U. Dixit,¹⁸ Ø. Djuvsland,²⁰ U. Dmitrieva,¹⁴⁰ A. Dobrin,⁶² B. Dönigus,⁶³
A. K. Dubey,¹³² J. M. Dubinski,¹³³ A. Dubla,⁹⁸ S. Dudi,⁹⁰ P. Dupieux,¹²⁵ M. Durkac,¹⁰⁶ N. Dzalaiova,¹²
T. M. Eder,¹³⁵ R. J. Ehlers,⁸⁷ V. N. Eikeland,²⁰ F. Eisenhut,⁶³ D. Elia,⁴⁹ B. Erasmus,¹⁰⁴ F. Ercolessi,²⁵
F. Erhardt,⁸⁹ M. R. Ersdal,²⁰ B. Espagnon,⁷² G. Eulisse,³² D. Evans,¹⁰¹ S. Evdokimov,¹⁴⁰ L. Fabbietti,⁹⁶
M. Faggin,²⁷ J. Faivre,⁷³ F. Fan,⁶ W. Fan,⁷⁴ A. Fantoni,⁴⁸ M. Fasel,⁸⁷ P. Feccchio,²⁹ A. Feliciello,⁵⁵
G. Feofilov,¹⁴⁰ A. Fernández Téllez,⁴⁴ M. B. Ferrer,³² A. Ferrero,¹²⁸ C. Ferrero,⁵⁵ A. Ferretti,²⁴
V. J. G. Feuillard,⁹⁵ V. Filova,³⁵ D. Finogeev,¹⁴⁰ F. M. Fionda,⁵¹ F. Flor,¹¹⁴ A. N. Flores,¹⁰⁸ S. Foertsch,⁶⁷
I. Fokin,⁹⁵ S. Fokin,¹⁴⁰ E. Fragiaco,⁵⁶ E. Frajna,¹³⁶ U. Fuchs,³² N. Funicello,²⁸ C. Furget,⁷³ A. Furs,¹⁴⁰
T. Fusayasu,⁹⁹ J. J. Gaardhøje,⁸³ M. Gagliardi,²⁴ A. M. Gago,¹⁰² C. D. Galvan,¹⁰⁹ D. R. Gangadharan,¹¹⁴
P. Ganoti,⁷⁸ C. Garabatos,⁹⁸ J. R. A. Garcia,⁴⁴ E. Garcia-Solis,⁹ K. Garg,¹⁰⁴ C. Gargiulo,³² A. Garibli,⁸¹
K. Garner,¹³⁵ A. Gautam,¹¹⁶ M. B. Gay Ducati,⁶⁵ M. Germain,¹⁰⁴ C. Ghosh,¹³² S. K. Ghosh,⁴ M. Giacalone,²⁵
P. Gianotti,⁴⁸ P. Giubellino,^{55,98} P. Giubilato,²⁷ A. M. C. Glaenger,¹²⁸ P. Glässel,⁹⁵ E. Glimos,¹²⁰ D. J. Q. Goh,⁷⁶
V. Gonzalez,¹³⁴ L. H. González-Trueba,⁶⁶ M. Gorgon,² S. Gotovac,³³ V. Grabski,⁶⁶ L. K. Graczykowski,¹³³
E. Grecka,⁸⁶ A. Grelli,⁵⁸ C. Grigoras,³² V. Grigoriev,¹⁴⁰ S. Grigoryan,^{1,141} F. Grosa,³²
J. F. Grosse-Oetringhaus,³² R. Grosso,⁹⁸ D. Grund,³⁵ G. G. Guardiano,¹¹¹ R. Guernane,⁷³ M. Guilbaud,¹⁰⁴
K. Gulbrandsen,⁸³ T. Gundem,⁶³ T. Gunji,¹²² W. Guo,⁶ A. Gupta,⁹¹ R. Gupta,⁹¹ S. P. Guzman,⁴⁴ L. Gyulai,¹³⁶
M. K. Habib,⁹⁸ C. Hadjidakis,⁷² H. Hamagaki,⁷⁶ M. Hamid,⁶ Y. Han,¹³⁸ R. Hannigan,¹⁰⁸ M. R. Haque,¹³³
J. W. Harris,¹³⁷ A. Harton,⁹ H. Hassan,⁸⁷ D. Hatzifotiadou,⁵⁰ P. Hauer,⁴² L. B. Havener,¹³⁷ S. T. Heckel,⁹⁶
E. Hellbär,⁹⁸ H. Helstrup,³⁴ M. Hemmer,⁶³ T. Herman,³⁵ G. Herrera Corral,⁸ F. Herrmann,¹³⁵ S. Herrmann,¹²⁶
K. F. Hetland,³⁴ B. Heybeck,⁶³ H. Hillemanns,³² C. Hills,¹¹⁷ B. Hippolyte,¹²⁷ B. Hofman,⁵⁸ B. Hohlweger,⁸⁴
J. Honermann,¹³⁵ G. H. Hong,¹³⁸ A. Horzyk,² R. Hosokawa,¹⁴ Y. Hou,⁶ P. Hristov,³² C. Hughes,¹²⁰ P. Huhn,⁶³
L. M. Huhta,¹¹⁵ C. V. Hulse,⁷² T. J. Humanic,⁸⁸ H. Hushnud,¹⁰⁰ A. Hutson,¹¹⁴ D. Hutter,³⁸ J. P. Iddon,¹¹⁷
R. Ilkaev,¹⁴⁰ H. Ilyas,¹³ M. Inaba,¹²³ G. M. Innocenti,³² M. Ippolitov,¹⁴⁰ A. Isakov,⁸⁶ T. Isidori,¹¹⁶
M. S. Islam,¹⁰⁰ M. Ivanov,¹² M. Ivanov,⁹⁸ V. Ivanov,¹⁴⁰ V. Izucheev,¹⁴⁰ M. Jablonski,² B. Jacak,⁷⁴ N. Jacazio,³²
P. M. Jacobs,⁷⁴ S. Jadlovská,¹⁰⁶ J. Jadlovsky,¹⁰⁶ S. Jaelani,⁸² L. Jaffe,³⁸ C. Jahnke,¹¹¹ M. J. Jakubowska,¹³³
M. A. Janik,¹³³ T. Janson,⁶⁹ M. Jercic,⁸⁹ O. Jevons,¹⁰¹ A. A. P. Jimenez,⁶⁴ F. Jonas,⁸⁷ P. G. Jones,¹⁰¹ J. M. Jowett,^{32,98}
J. Jung,⁶³ M. Jung,⁶³ A. Junique,³² A. Jusko,¹⁰¹ M. J. Kabus,^{32,133} J. Kaewjai,¹⁰⁵ P. Kalinak,⁵⁹ A. S. Kalteyer,⁹⁸
A. Kalweit,³² V. Kaplin,¹⁴⁰ A. Karasu Uysal,⁷¹ D. Karatovic,⁸⁹ O. Karavichev,¹⁴⁰ T. Karavicheva,¹⁴⁰
P. Karczmarczyk,¹³³ E. Karpechev,¹⁴⁰ V. Kashyap,⁸⁰ U. Keschull,⁶⁹ R. Keidel,¹³⁹ D. L. D. Keijdener,⁵⁸ M. Keil,³²
B. Ketzer,⁴² A. M. Khan,⁶ S. Khan,¹⁵ A. Khanzadeev,¹⁴⁰ Y. Kharlov,¹⁴⁰ A. Khatun,¹⁵ A. Khuntia,¹⁰⁷
B. Kileng,³⁴ B. Kim,¹⁶ C. Kim,¹⁶ D. J. Kim,¹¹⁵ E. J. Kim,⁶⁸ J. Kim,¹³⁸ J. S. Kim,⁴⁰ J. Kim,⁹⁵ J. Kim,⁶⁸
M. Kim,⁹⁵ S. Kim,¹⁷ T. Kim,¹³⁸ K. Kimura,⁹³ S. Kirsch,⁶³ I. Kisel,³⁸ S. Kiselev,¹⁴⁰ A. Kisiel,¹³³
J. P. Kitowski,² J. L. Klay,⁵ J. Klein,³² S. Klein,⁷⁴ C. Klein-Bösing,¹³⁵ M. Kleiner,⁶³ T. Klemenz,⁹⁶
A. Kluge,³² A. G. Knosp,¹¹⁴ C. Kobdaj,¹⁰⁵ T. Kollegger,⁹⁸ A. Kondratyev,¹⁴¹ E. Kondratyuk,¹⁴⁰ J. Konig,⁶³
S. A. Konigstorfer,⁹⁶ P. J. Konopka,³² G. Kornakov,¹³³ S. D. Koryciak,² A. Kotliarov,⁸⁶ O. Kovalenko,⁷⁹

V. Kovalenko¹⁴⁰ M. Kowalski¹⁰⁷ I. Králik⁵⁹ A. Kravčáková³⁷ L. Kreis⁹⁸ M. Krivda^{59,101} F. Krizek⁸⁶
 K. Krizkova Gajdosova³⁵ M. Kroesen⁹⁵ M. Krüger⁶³ D. M. Krupova³⁵ E. Kryshen¹⁴⁰ V. Kučera³²
 C. Kuhn¹²⁷ P. G. Kuijer⁸⁴ T. Kumaoka¹²³ D. Kumar¹³² L. Kumar⁹⁰ N. Kumar⁹⁰ S. Kumar³¹ S. Kundu³²
 P. Kurashvili⁷⁹ A. Kurepin¹⁴⁰ A. B. Kurepin¹⁴⁰ S. Kushpil⁸⁶ J. Kvapil¹⁰¹ M. J. Kweon⁵⁷ J. Y. Kwon⁵⁷
 Y. Kwon¹³⁸ S. L. La Pointe³⁸ P. La Rocca²⁶ Y. S. Lai⁷⁴ A. Lakrathok¹⁰⁵ M. Lamanna³² R. Langoy¹¹⁹
 P. Larionov³² E. Laudi³² L. Lautner^{32,96} R. Lavicka¹⁰³ T. Lazareva¹⁴⁰ R. Lea^{54,131} G. Legras¹³⁵
 J. Lehrbach³⁸ R. C. Lemmon⁸⁵ I. León Monzón¹⁰⁹ M. M. Lesch⁹⁶ E. D. Lesser¹⁸ M. Lettrich⁹⁶ P. Lévai¹³⁶
 X. Li¹⁰ X. L. Li⁶ J. Lien¹¹⁹ R. Lietava¹⁰¹ B. Lim¹⁶ S. H. Lim¹⁶ V. Lindenstruth³⁸ A. Lindner⁴⁵
 C. Lippmann⁹⁸ A. Liu¹⁸ D. H. Liu⁶ J. Liu¹¹⁷ I. M. Lofnes²⁰ C. Loizides⁸⁷ P. Loncar³³ J. A. Lopez⁹⁵
 X. Lopez¹²⁵ E. López Torres⁷ P. Lu^{98,118} J. R. Luhder¹³⁵ M. Lunardon²⁷ G. Luparello⁵⁶ Y. G. Ma³⁹
 A. Maevskaya¹⁴⁰ M. Mager³² T. Mahmoud⁴² A. Maire¹²⁷ M. Malaev¹⁴⁰ G. Malfattore²⁵ N. M. Malik⁹¹
 Q. W. Malik¹⁹ S. K. Malik⁹¹ L. Malinina^{141,g} D. Mal'Kevich¹⁴⁰ D. Mallick⁸⁰ N. Mallick⁴⁷ G. Mandaglio^{30,52}
 V. Manko¹⁴⁰ F. Manso¹²⁵ V. Manzari⁴⁹ Y. Mao⁶ G. V. Margagliotti²³ A. Margotti⁵⁰ A. Marín⁹⁸
 C. Markert¹⁰⁸ P. Martinengo³² J. L. Martinez¹¹⁴ M. I. Martínez⁴⁴ G. Martínez García¹⁰⁴ S. Masciocchi⁹⁸
 M. Maserà²⁴ A. Masoni⁵¹ L. Massacrier⁷² A. Mastroserio^{49,129} A. M. Mathis⁹⁶ O. Matonoha⁷⁵
 P. F. T. Matuoka¹¹⁰ A. Matyja¹⁰⁷ C. Mayer¹⁰⁷ A. L. Mazuecos³² F. Mazzaschi²⁴ M. Mazzilli³² J. E. Mdhluhi¹²¹
 A. F. Mechler⁶³ Y. Melikyan¹⁴⁰ A. Menchaca-Rocha⁶⁶ E. Meninno^{28,103} A. S. Menon¹¹⁴ M. Meres¹²
 S. Mhlanga^{67,113} Y. Miake¹²³ L. Micheletti⁵⁵ L. C. Migliorin¹²⁶ D. L. Mihaylov⁹⁶ K. Mikhaylov^{140,141}
 A. N. Mishra¹³⁶ D. Miśkowiec⁹⁸ A. Modak⁴ A. P. Mohanty⁵⁸ B. Mohanty⁸⁰ M. Mohisin Khan^{15,e}
 M. A. Molander⁴³ Z. Moravcova⁸³ C. Mordasini⁹⁶ D. A. Moreira De Godoy¹³⁵ I. Morozov¹⁴⁰ A. Morsch³²
 T. Mrnjavac³² V. Muccifora⁴⁸ S. Muhuri¹³² J. D. Mulligan⁷⁴ A. Mulliri²² M. G. Munhoz¹¹⁰ R. H. Munzer⁶³
 H. Murakami¹²² S. Murray¹¹³ L. Musa³² J. Musinsky⁵⁹ J. W. Myrcha¹³³ B. Naik¹²¹ R. Nair⁷⁹
 A. I. Nambrath¹⁸ B. K. Nandi⁴⁶ R. Nania⁵⁰ E. Nappi⁴⁹ A. F. Nassirpour⁷⁵ A. Nath⁹⁵ C. Natrass¹²⁰
 A. Neagu¹⁹ A. Negru¹²⁴ L. Nellen⁶⁴ S. V. Nesbo³⁴ G. Neskovic³⁸ D. Nesterov¹⁴⁰ B. S. Nielsen⁸³
 E. G. Nielsen⁸³ S. Nikolaev¹⁴⁰ S. Nikulin¹⁴⁰ V. Nikulin¹⁴⁰ F. Noferini⁵⁰ S. Noh¹¹ P. Nomokonov¹⁴¹
 J. Norman¹¹⁷ N. Novitzky¹²³ P. Nowakowski¹³³ A. Nyanin¹⁴⁰ J. Nystrand²⁰ M. Ogino⁷⁶ A. Ohlson⁷⁵
 V. A. Okorokov¹⁴⁰ J. Oleniacz¹³³ A. C. Oliveira Da Silva¹²⁰ M. H. Oliver¹³⁷ A. Onnerstad¹¹⁵ C. Oppedisano⁵⁵
 A. Ortiz Velasquez⁶⁴ A. Oskarsson⁷⁵ J. Otwinowski¹⁰⁷ M. Oya⁹³ K. Oyama⁷⁶ Y. Pachmayer⁹⁵ S. Padhan⁴⁶
 D. Pagano^{54,131} G. Paić⁶⁴ A. Palasciano⁴⁹ S. Panebianco¹²⁸ H. Park¹²³ J. Park⁵⁷ J. E. Parkkila³²
 R. N. Patra⁹¹ B. Paul²² H. Pei⁶ T. Peitzmann⁵⁸ X. Peng⁶ M. Pennisi²⁴ L. G. Pereira⁶⁵ H. Pereira Da Costa¹²⁸
 D. Peresunko¹⁴⁰ G. M. Perez⁷ S. Perrin¹²⁸ Y. Pestov¹⁴⁰ V. Petráček³⁵ V. Petrov¹⁴⁰ M. Petrovici⁴⁵
 R. P. Pezzi^{65,104} S. Piano⁵⁶ M. Pikna¹² P. Pillot¹⁰⁴ O. Pinazza^{32,50} L. Pinsky¹¹⁴ C. Pinto⁹⁶ S. Pisano⁴⁸
 M. Płoskoń⁷⁴ M. Planinic⁸⁹ F. Pliquet⁶³ M. G. Poghosyan⁸⁷ S. Politano²⁹ N. Poljak⁸⁹ A. Pop⁴⁵
 S. Porteboeuf-Houssais¹²⁵ J. Porter⁷⁴ V. Pozdniakov¹⁴¹ S. K. Prasad⁴ S. Prasad⁴⁷ R. Preghenella⁵⁰
 F. Prino⁵⁵ C. A. Pruneau¹³⁴ I. Pshenichnov¹⁴⁰ M. Puccio³² S. Pucillo²⁴ Z. Pugelova¹⁰⁶ S. Qiu⁸⁴
 L. Quaglia²⁴ R. E. Quishpe¹¹⁴ S. Ragoni^{14,101} A. Rakotozafindrabe¹²⁸ L. Ramello^{55,130} F. Rami¹²⁷
 S. A. R. Ramirez⁴⁴ T. A. Rancien⁷³ R. Raniwala⁹² S. Raniwala⁹² M. Rasa²⁶ S. S. Räsänen⁴³ R. Rath^{47,50}
 I. Ravasenga⁸⁴ K. F. Read^{87,120} C. Reckziegel¹¹² A. R. Redelbach³⁸ K. Redlich^{79,f} A. Rehman²⁰ F. Reidt³²
 H. A. Reme-Ness³⁴ Z. Rescakova³⁷ K. Reygers⁹⁵ A. Riabov¹⁴⁰ V. Riabov¹⁴⁰ R. Ricci²⁸ T. Richert⁷⁵
 M. Richter¹⁹ A. A. Riedel⁹⁶ W. Riegler³² F. Riggi²⁶ C. Ristea⁶² M. Rodríguez Cahuantzi⁴⁴ K. Røed¹⁹
 R. Rogalev¹⁴⁰ E. Rogochaya¹⁴¹ T. S. Rogoschinski⁶³ D. Rohr³² D. Röhrich²⁰ P. F. Rojas⁴⁴ S. Rojas Torres³⁵
 P. S. Rokita¹³³ G. Romanenko¹⁴¹ F. Ronchetti⁴⁸ A. Rosano^{30,52} E. D. Rosas⁶⁴ A. Rossi⁵³ A. Roy⁴⁷ P. Roy¹⁰⁰
 S. Roy⁴⁶ N. Rubini²⁵ O. V. Rueda⁷⁵ D. Ruggiano¹³³ R. Rui²³ B. Rumyantsev¹⁴¹ P. G. Russek² R. Russo⁸⁴
 A. Rustamov⁸¹ E. Ryabinkin¹⁴⁰ Y. Ryabov¹⁴⁰ A. Rybicki¹⁰⁷ H. Rytkonen¹¹⁵ W. Rzeska¹³³
 O. A. M. Saarimaki⁴³ R. Sadek¹⁰⁴ S. Sadhu³¹ S. Sadovsky¹⁴⁰ J. Saetre²⁰ K. Šafařík³⁵ S. K. Saha⁴
 S. Saha⁸⁰ B. Sahoo⁴⁶ R. Sahoo⁴⁷ S. Sahoo⁶⁰ D. Sahu⁴⁷ P. K. Sahu⁶⁰ J. Saini¹³² K. Sajdakova³⁷ S. Sakai¹²³
 M. P. Salvan⁹⁸ S. Sambyal⁹¹ T. B. Saramela¹¹⁰ D. Sarkar¹³⁴ N. Sarkar¹³² P. Sarma⁴¹ V. Sarritzu²²
 V. M. Sarti⁹⁶ M. H. P. Sas¹³⁷ J. Schambach⁸⁷ H. S. Scheid⁶³ C. Schiaua⁴⁵ R. Schicker⁹⁵ A. Schmah⁹⁵
 C. Schmidt⁹⁸ H. R. Schmidt⁹⁴ M. O. Schmidt³² M. Schmidt⁹⁴ N. V. Schmidt⁸⁷ A. R. Schmier¹²⁰ R. Schotter¹²⁷

J. Schukraft³², K. Schwarz⁹⁸, K. Schweda⁹⁸, G. Scioli²⁵, E. Scomparin⁵⁵, J. E. Seger¹⁴, Y. Sekiguchi¹²²,
 D. Sekihata¹²², I. Selyuzhenkov^{98,140}, S. Senyukov¹²⁷, J. J. Seo⁵⁷, D. Serebryakov¹⁴⁰, L. Šerkšnytė⁹⁶,
 A. Sevcenco⁶², T. J. Shaba⁶⁷, A. Shabetai¹⁰⁴, R. Shahoyan³², A. Shangaraev¹⁴⁰, A. Sharma⁹⁰, D. Sharma⁴⁶,
 H. Sharma¹⁰⁷, M. Sharma⁹¹, N. Sharma⁹⁰, S. Sharma⁷⁶, S. Sharma⁹¹, U. Sharma⁹¹, A. Shatat⁷², O. Sheibani¹¹⁴,
 K. Shigaki⁹³, M. Shimomura⁷⁷, S. Shirinkin¹⁴⁰, Q. Shou³⁹, Y. Sibiraki¹⁴⁰, S. Siddhanta⁵¹, T. Siemiarz⁷⁹,
 T. F. Silva¹¹⁰, D. Silvermyr⁷⁵, T. Simantathammakul¹⁰⁵, R. Simeonov³⁶, B. Singh⁹¹, B. Singh⁹⁶, R. Singh⁸⁰,
 R. Singh⁹¹, R. Singh⁴⁷, S. Singh¹⁵, V. K. Singh¹³², V. Singhal¹³², T. Sinha¹⁰⁰, B. Sitar¹², M. Sitta^{55,130},
 T. B. Skaali¹⁹, G. Skorodumovs⁹⁵, M. Slupecki⁴³, N. Smirnov¹³⁷, R. J. M. Snellings⁵⁸, E. H. Solheim¹⁹,
 J. Song¹¹⁴, A. Songmoolnak¹⁰⁵, F. Soramel²⁷, S. Sorensen¹²⁰, R. Spijkers⁸⁴, I. Sputowska¹⁰⁷, J. Staa⁷⁵,
 J. Stachel⁹⁵, I. Stan⁶², P. J. Steffanic¹²⁰, S. F. Stiefelmaier⁹⁵, D. Stocco¹⁰⁴, I. Storehaug¹⁹, M. M. Storetvedt³⁴,
 P. Stratmann¹³⁵, S. Strazzi²⁵, C. P. Stylianidis⁸⁴, A. A. P. Suaide¹¹⁰, C. Suire⁷², M. Sukhanov¹⁴⁰, M. Suljic³²,
 V. Sumberia⁹¹, S. Sumowidagdo⁸², S. Swain⁶⁰, I. Szarka¹², U. Tabassam¹³, S. F. Taghavi⁹⁶, G. Taillepiéd⁹⁸,
 J. Takahashi¹¹¹, G. J. Tambave²⁰, S. Tang^{6,125}, Z. Tang¹¹⁸, J. D. Tapia Takaki¹¹⁶, N. Tapus¹²⁴,
 L. A. Tarasovicova¹³⁵, M. G. Tazila⁴⁵, G. F. Tassielli³¹, A. Tauro³², A. Telesca³², L. Terlizzi²⁴, C. Terrevoli¹¹⁴,
 G. Tersimonov³, S. Thakur⁴, D. Thomas¹⁰⁸, A. Tikhonov¹⁴⁰, A. R. Timmins¹¹⁴, M. Tkacik¹⁰⁶, T. Tkacik¹⁰⁶,
 A. Toia⁶³, R. Tokumoto⁹³, N. Topilskaya¹⁴⁰, M. Toppi⁴⁸, F. Torales-Acosta¹⁸, T. Tork⁷², A. G. Torres Ramos³¹,
 A. Trifiró^{30,52}, A. S. Triolo^{30,52}, S. Tripathy⁵⁰, T. Tripathy⁴⁶, S. Trogolo³², V. Trubnikov³, W. H. Trzaska¹¹⁵,
 T. P. Trzcinski¹³³, R. Turrisi⁵³, T. S. Tveter¹⁹, K. Ullaland²⁰, B. Ulukutlu⁹⁶, A. Uras¹²⁶, M. Urioni^{54,131},
 G. L. Usai²², M. Vala³⁷, N. Valle²¹, S. Vallerio⁵⁵, L. V. R. van Doremalen⁵⁸, M. van Leeuwen⁸⁴, C. A. van Veen⁹⁵,
 R. J. G. van Weelden⁸⁴, P. Vande Vyvre³², D. Varga¹³⁶, Z. Varga¹³⁶, M. Varga-Kofarago¹³⁶, M. Vasileiou⁷⁸,
 A. Vasiliev¹⁴⁰, O. Vázquez Doce⁴⁸, V. Vechernin¹⁴⁰, E. Vercellin²⁴, S. Vergara Limón⁴⁴, L. Vermunt⁹⁸,
 R. Vértési¹³⁶, M. Verweij⁵⁸, L. Vickovic³³, Z. Vilakazi¹²¹, O. Villalobos Baillie¹⁰¹, G. Vino⁴⁹, A. Vinogradov¹⁴⁰,
 T. Virgili²⁸, V. Vislavicius⁸³, A. Vodopyanov¹⁴¹, B. Volkel³², M. A. Völkl⁹⁵, K. Voloshin¹⁴⁰, S. A. Voloshin¹³⁴,
 G. Volpe³¹, B. von Haller³², I. Vorobyev⁹⁶, N. Vozniuk¹⁴⁰, J. Vrláková³⁷, B. Wagner²⁰, C. Wang³⁹, D. Wang³⁹,
 A. Wegrzynek³², F. T. Weiglhofer³⁸, S. C. Wenzel³², J. P. Wessels¹³⁵, S. L. Weyhmiller¹³⁷, J. Wiechula⁶³,
 J. Wikne¹⁹, G. Wilk⁷⁹, J. Wilkinson⁹⁸, G. A. Willems¹³⁵, B. Windelband⁹⁵, M. Winn¹²⁸, J. R. Wright¹⁰⁸,
 W. Wu³⁹, Y. Wu¹¹⁸, R. Xu⁶, A. Yadav⁴², A. K. Yadav¹³², S. Yalcin⁷¹, Y. Yamaguchi⁹³, K. Yamakawa⁹³, S. Yang²⁰,
 S. Yano⁹³, Z. Yin⁶, I.-K. Yoo¹⁶, J. H. Yoon⁵⁷, S. Yuan²⁰, A. Yuncu⁹⁵, V. Zaccolo²³, C. Zampolli³²,
 H. J. C. Zanoli⁵⁸, F. Zanone⁹⁵, N. Zardoshti^{32,101}, A. Zarochentsev¹⁴⁰, P. Závada⁶¹, N. Zaviyalov¹⁴⁰, M. Zhalov¹⁴⁰,
 B. Zhang⁶, S. Zhang³⁹, X. Zhang⁶, Y. Zhang¹¹⁸, Z. Zhang⁶, M. Zhao¹⁰, V. Zhrebchevskii¹⁴⁰, Y. Zhi¹⁰,
 N. Zhigareva¹⁴⁰, D. Zhou⁶, Y. Zhou⁸³, J. Zhu^{6,98}, Y. Zhu⁶, G. Zinovjev^{3,a} and N. Zurlo^{54,131}

(ALICE Collaboration)

¹A.I. Alikhanyan National Science Laboratory (Yerevan Physics Institute) Foundation, Yerevan, Armenia

²AGH University of Science and Technology, Cracow, Poland

³Bogolyubov Institute for Theoretical Physics, National Academy of Sciences of Ukraine, Kiev, Ukraine

⁴Bose Institute, Department of Physics and Centre for Astroparticle Physics and Space Science (CAPSS), Kolkata, India

⁵California Polytechnic State University, San Luis Obispo, California, USA

⁶Central China Normal University, Wuhan, China

⁷Centro de Aplicaciones Tecnológicas y Desarrollo Nuclear (CEADEN), Havana, Cuba

⁸Centro de Investigación y de Estudios Avanzados (CINVESTAV), Mexico City and Mérida, Mexico

⁹Chicago State University, Chicago, Illinois, USA

¹⁰China Institute of Atomic Energy, Beijing, China

¹¹Chungbuk National University, Cheongju, Republic of Korea

¹²Comenius University Bratislava, Faculty of Mathematics, Physics and Informatics, Bratislava, Slovak Republic

¹³COMSATS University Islamabad, Islamabad, Pakistan

¹⁴Creighton University, Omaha, Nebraska, USA

¹⁵Department of Physics, Aligarh Muslim University, Aligarh, India

¹⁶Department of Physics, Pusan National University, Pusan, Republic of Korea

¹⁷Department of Physics, Sejong University, Seoul, Republic of Korea

- ¹⁸*Department of Physics, University of California, Berkeley, California, USA*
- ¹⁹*Department of Physics, University of Oslo, Oslo, Norway*
- ²⁰*Department of Physics and Technology, University of Bergen, Bergen, Norway*
- ²¹*Dipartimento di Fisica, Università di Pavia, Pavia, Italy*
- ²²*Dipartimento di Fisica dell'Università and Sezione INFN, Cagliari, Italy*
- ²³*Dipartimento di Fisica dell'Università and Sezione INFN, Trieste, Italy*
- ²⁴*Dipartimento di Fisica dell'Università and Sezione INFN, Turin, Italy*
- ²⁵*Dipartimento di Fisica e Astronomia dell'Università and Sezione INFN, Bologna, Italy*
- ²⁶*Dipartimento di Fisica e Astronomia dell'Università and Sezione INFN, Catania, Italy*
- ²⁷*Dipartimento di Fisica e Astronomia dell'Università and Sezione INFN, Padova, Italy*
- ²⁸*Dipartimento di Fisica "E.R. Caianiello" dell'Università and Gruppo Collegato INFN, Salerno, Italy*
- ²⁹*Dipartimento DISAT del Politecnico and Sezione INFN, Turin, Italy*
- ³⁰*Dipartimento di Scienze MIFT, Università di Messina, Messina, Italy*
- ³¹*Dipartimento Interateneo di Fisica "M. Merlin" and Sezione INFN, Bari, Italy*
- ³²*European Organization for Nuclear Research (CERN), Geneva, Switzerland*
- ³³*Faculty of Electrical Engineering, Mechanical Engineering and Naval Architecture, University of Split, Split, Croatia*
- ³⁴*Faculty of Engineering and Science, Western Norway University of Applied Sciences, Bergen, Norway*
- ³⁵*Faculty of Nuclear Sciences and Physical Engineering, Czech Technical University in Prague, Prague, Czech*
- ³⁶*Faculty of Physics, Sofia University, Sofia, Bulgaria*
- ³⁷*Faculty of Science, P.J. Šafárik University, Košice, Slovak Republic*
- ³⁸*Frankfurt Institute for Advanced Studies, Johann Wolfgang Goethe-Universität Frankfurt, Frankfurt, Germany*
- ³⁹*Fudan University, Shanghai, China*
- ⁴⁰*Gangneung-Wonju National University, Gangneung, Republic of Korea*
- ⁴¹*Gauhati University, Department of Physics, Guwahati, India*
- ⁴²*Helmholtz-Institut für Strahlen- und Kernphysik, Rheinische Friedrich-Wilhelms-Universität Bonn, Bonn, Germany*
- ⁴³*Helsinki Institute of Physics (HIP), Helsinki, Finland*
- ⁴⁴*High Energy Physics Group, Universidad Autónoma de Puebla, Puebla, Mexico*
- ⁴⁵*Horia Hulubei National Institute of Physics and Nuclear Engineering, Bucharest, Romania*
- ⁴⁶*Indian Institute of Technology Bombay (IIT), Mumbai, India*
- ⁴⁷*Indian Institute of Technology Indore, Indore, India*
- ⁴⁸*INFN, Laboratori Nazionali di Frascati, Frascati, Italy*
- ⁴⁹*INFN, Sezione di Bari, Bari, Italy*
- ⁵⁰*INFN, Sezione di Bologna, Bologna, Italy*
- ⁵¹*INFN, Sezione di Cagliari, Cagliari, Italy*
- ⁵²*INFN, Sezione di Catania, Catania, Italy*
- ⁵³*INFN, Sezione di Padova, Padova, Italy*
- ⁵⁴*INFN, Sezione di Pavia, Pavia, Italy*
- ⁵⁵*INFN, Sezione di Torino, Turin, Italy*
- ⁵⁶*INFN, Sezione di Trieste, Trieste, Italy*
- ⁵⁷*Inha University, Incheon, Republic of Korea*
- ⁵⁸*Institute for Gravitational and Subatomic Physics (GRASP), Utrecht University/Nikhef, Utrecht, Netherlands*
- ⁵⁹*Institute of Experimental Physics, Slovak Academy of Sciences, Košice, Slovak Republic*
- ⁶⁰*Institute of Physics, Homi Bhabha National Institute, Bhubaneswar, India*
- ⁶¹*Institute of Physics of the Czech Academy of Sciences, Prague, Czech Republic*
- ⁶²*Institute of Space Science (ISS), Bucharest, Romania*
- ⁶³*Institut für Kernphysik, Johann Wolfgang Goethe-Universität Frankfurt, Frankfurt, Germany*
- ⁶⁴*Instituto de Ciencias Nucleares, Universidad Nacional Autónoma de México, Mexico City, Mexico*
- ⁶⁵*Instituto de Física, Universidade Federal do Rio Grande do Sul (UFRGS), Porto Alegre, Brazil*
- ⁶⁶*Instituto de Física, Universidad Nacional Autónoma de México, Mexico City, Mexico*
- ⁶⁷*iThemba LABS, National Research Foundation, Somerset West, South Africa*
- ⁶⁸*Jeonbuk National University, Jeonju, Republic of Korea*
- ⁶⁹*Johann-Wolfgang-Goethe Universität Frankfurt Institut für Informatik, Fachbereich Informatik und Mathematik, Frankfurt, Germany*
- ⁷⁰*Korea Institute of Science and Technology Information, Daejeon, Republic of Korea*
- ⁷¹*KTO Karatay University, Konya, Turkey*
- ⁷²*Laboratoire de Physique des 2 Infinis, Irène Joliot-Curie, Orsay, France*
- ⁷³*Laboratoire de Physique Subatomique et de Cosmologie, Université Grenoble-Alpes, CNRS-IN2P3, Grenoble, France*
- ⁷⁴*Lawrence Berkeley National Laboratory, Berkeley, California, USA*
- ⁷⁵*Lund University Department of Physics, Division of Particle Physics, Lund, Sweden*
- ⁷⁶*Nagasaki Institute of Applied Science, Nagasaki, Japan*
- ⁷⁷*Nara Women's University (NWU), Nara, Japan*

- ⁷⁸*National and Kapodistrian University of Athens, School of Science, Department of Physics, Athens, Greece*
- ⁷⁹*National Centre for Nuclear Research, Warsaw, Poland*
- ⁸⁰*National Institute of Science Education and Research, Homi Bhabha National Institute, Jatni, India*
- ⁸¹*National Nuclear Research Center, Baku, Azerbaijan*
- ⁸²*National Research and Innovation Agency - BRIN, Jakarta, Indonesia*
- ⁸³*Niels Bohr Institute, University of Copenhagen, Copenhagen, Denmark*
- ⁸⁴*Nikhef, National Institute for Subatomic Physics, Amsterdam, Netherlands*
- ⁸⁵*Nuclear Physics Group, STFC Daresbury Laboratory, Daresbury, United Kingdom*
- ⁸⁶*Nuclear Physics Institute of the Czech Academy of Sciences, Husinec-Řež, Czech Republic*
- ⁸⁷*Oak Ridge National Laboratory, Oak Ridge, Tennessee, USA*
- ⁸⁸*Ohio State University, Columbus, Ohio, USA*
- ⁸⁹*Physics Department, Faculty of Science, University of Zagreb, Zagreb, Croatia*
- ⁹⁰*Physics Department, Panjab University, Chandigarh, India*
- ⁹¹*Physics Department, University of Jammu, Jammu, India*
- ⁹²*Physics Department, University of Rajasthan, Jaipur, India*
- ⁹³*Physics Program and International Institute for Sustainability with Knotted Chiral Meta Matter (SKCM2), Hiroshima University, Hiroshima, Japan*
- ⁹⁴*Physikalisches Institut, Eberhard-Karls-Universität Tübingen, Tübingen, Germany*
- ⁹⁵*Physikalisches Institut, Ruprecht-Karls-Universität Heidelberg, Heidelberg, Germany*
- ⁹⁶*Physik Department, Technische Universität München, Munich, Germany*
- ⁹⁷*Politecnico di Bari and Sezione INFN, Bari, Italy*
- ⁹⁸*Research Division and ExtreMe Matter Institute EMMI, GSI Helmholtzzentrum für Schwerionenforschung GmbH, Darmstadt, Germany*
- ⁹⁹*Saga University, Saga, Japan*
- ¹⁰⁰*Saha Institute of Nuclear Physics, Homi Bhabha National Institute, Kolkata, India*
- ¹⁰¹*School of Physics and Astronomy, University of Birmingham, Birmingham, United Kingdom*
- ¹⁰²*Sección Física, Departamento de Ciencias, Pontificia Universidad Católica del Perú, Lima, Peru*
- ¹⁰³*Stefan Meyer Institut für Subatomare Physik (SMI), Vienna, Austria*
- ¹⁰⁴*SUBATECH, IMT Atlantique, Nantes Université, CNRS-IN2P3, Nantes, France*
- ¹⁰⁵*Suranaree University of Technology, Nakhon Ratchasima, Thailand*
- ¹⁰⁶*Technical University of Košice, Košice, Slovak Republic*
- ¹⁰⁷*The Henryk Niewodniczanski Institute of Nuclear Physics, Polish Academy of Sciences, Cracow, Poland*
- ¹⁰⁸*The University of Texas at Austin, Austin, Texas, USA*
- ¹⁰⁹*Universidad Autónoma de Sinaloa, Culiacán, Mexico*
- ¹¹⁰*Universidade de São Paulo (USP), São Paulo, Brazil*
- ¹¹¹*Universidade Estadual de Campinas (UNICAMP), Campinas, Brazil*
- ¹¹²*Universidade Federal do ABC, Santo Andre, Brazil*
- ¹¹³*University of Cape Town, Cape Town, South Africa*
- ¹¹⁴*University of Houston, Houston, Texas, USA*
- ¹¹⁵*University of Jyväskylä, Jyväskylä, Finland*
- ¹¹⁶*University of Kansas, Lawrence, Kansas, USA*
- ¹¹⁷*University of Liverpool, Liverpool, United Kingdom*
- ¹¹⁸*University of Science and Technology of China, Hefei, China*
- ¹¹⁹*University of South-Eastern Norway, Kongsberg, Norway*
- ¹²⁰*University of Tennessee, Knoxville, Tennessee, USA*
- ¹²¹*University of the Witwatersrand, Johannesburg, South Africa*
- ¹²²*University of Tokyo, Tokyo, Japan*
- ¹²³*University of Tsukuba, Tsukuba, Japan*
- ¹²⁴*University Politehnica of Bucharest, Bucharest, Romania*
- ¹²⁵*Université Clermont Auvergne, CNRS/IN2P3, LPC, Clermont-Ferrand, France*
- ¹²⁶*Université de Lyon, CNRS/IN2P3, Institut de Physique des 2 Infinis de Lyon, Lyon, France*
- ¹²⁷*Université de Strasbourg, CNRS, IPHC UMR 7178, F-67000 Strasbourg, France*
- ¹²⁸*Université Paris-Saclay Centre d'Etudes de Saclay (CEA), IRFU, Département de Physique Nucléaire (DPhN), Saclay, France*
- ¹²⁹*Università degli Studi di Foggia, Foggia, Italy*
- ¹³⁰*Università del Piemonte Orientale, Vercelli, Italy*
- ¹³¹*Università di Brescia, Brescia, Italy*
- ¹³²*Variable Energy Cyclotron Centre, Homi Bhabha National Institute, Kolkata, India*
- ¹³³*Warsaw University of Technology, Warsaw, Poland*
- ¹³⁴*Wayne State University, Detroit, Michigan, USA*
- ¹³⁵*Westfälische Wilhelms-Universität Münster, Institut für Kernphysik, Münster, Germany*

¹³⁶*Wigner Research Centre for Physics, Budapest, Hungary*

¹³⁷*Yale University, New Haven, Connecticut, USA*

¹³⁸*Yonsei University, Seoul, Republic of Korea*

¹³⁹*Zentrum für Technologie und Transfer (ZTT), Worms, Germany*

¹⁴⁰*Affiliated with an institute covered by a cooperation agreement with CERN*

¹⁴¹*Affiliated with an international laboratory covered by a cooperation agreement with CERN*

^aDeceased.

^bAlso at Max-Planck-Institut für Physik, Munich, Germany.

^cAlso at Italian National Agency for New Technologies, Energy and Sustainable Economic Development (ENEA), Bologna, Italy.

^dAlso at Dipartimento DET del Politecnico di Torino, Turin, Italy.

^eAlso at Department of Applied Physics, Aligarh Muslim University, Aligarh, India.

^fAlso at Institute of Theoretical Physics, University of Wrocław, Wrocław, Poland.

^gAlso at an institution covered by a cooperation agreement with CERN.